Journal of Drug Delivery Science and Technology 86 (2023) 104640

Contents lists available at ScienceDirect

Journal of Drug Delivery Science and Technology

journal homepage: www.elsevier.com/locate/jddst

Effect of nozzle shape and applied load on jet injection efficiency

Whitney Tran, Cormak Weeks [1], Yatish Rane [2], Jeremy Marston [*]

Department of Chemical Engineering, Texas Tech University, Lubbock, TX, 79409, USA

A B S T R A C T

In this paper we present new results on jet injection with the overall aim of providing an efficient drug delivery into the intradermal region of the skin. To advance upon previous work in this area, we studied the use of various geometries for the nozzle (ampule) tip, which is applied to the skin. The geometries included a regular (flat-top) nozzle, tapered nozzles (conical and parabolic), and one wide base nozzle in order to vary the local stress in the skin layers directly beneath the injector. In all of these geometries, we also varied both the applied load and the skin support (e.g., solid backing vs. porcine tissue). We found that the use of applied load combined with a wider contact area led to more consistent injections with dispersion characteristics that may be preferable for vaccinations utilizing skin-based electroporation.

1. Introduction

Jet injection is becoming an attractive needle-free alternative to standard hypodermic injections for a number of reasons. Chief among these are: elimination of needle-phobia in patients [1–3], improved patient compliance, reduction in sharps waste [4,5] and occurrence of accidental needle-stick injuries [6–8], and proven efficacy in terms of immunogenecity [9–16], especially for fractional dose vaccinations [17–20].

The basic premise of needle-free jet injection relies upon creating a highly pressurized liquid in an ampule (or cartridge) with a narrow orifice (typically $d \sim O(100)\mu$m) to yield a high-speed jet ($v_j \sim O(100)$ m/s) that can puncture the skin and deposit drug to the target tissue below[1,21] (e.g., dermis, subcutaneous, or intramuscular). A summary of various mechanisms and corresponding injection volumes and penetration depths can be found in a recent review by Schoppink & Rivas [22].

Whilst many studies in the literature focus on systematic variation of parameters such as orifice diameter[21,23,24], jet speed [21–25], fluid viscosity [26,27], substrate or skin stiffness [28,29], etc., few have reported on the effect of the ampule or nozzle design [30,31], specifically the part which contacts the skin. This component is crucial since, along with the applied load, it will determine the distribution of stress within the tissue layers beneath the skin. Furthermore, since novel injector designs aim to incorporate skin tensioning mechanisms [32] and vacuums via use of a shroud [33–36], this component becomes even more important. In particular, the use of a shroud is pertinent in light of a recent study into the production of aerosols from jet injection [37]. The effects of loading and skin tension have been known for some time [32,38,39], but have not been well studied or quantified, with the exception of Rohilla et al. [40].

Furthermore, since the exact dimensions of the ampule (or nozzle) and/or shroud will vary from one injector to another, it is prudent to assess the effect of this component. Motivation also stems from design of novel injectors that aim to couple injection with skin-based electroporation (EP) modules [41,42], wherein it is sought after to enhance the electric field distribution. As such, we focused herein on the effect of the geometry of the nozzle tip and the spacer attachment (which may be incorporated in some injectors as the 'ampule' or 'shroud') on delivery efficacy and fluid distribution. Specifically, we assessed the coupled effect of the geometry and applied load. In addition, the substrate underneath the skin tissues was varied to compare how the stiffness, and subsequently local compression, affects the injection.

2. Methods

Skin samples: Human skin samples from a batch purchased from the National Disease Research Interchange (NDRI), were selected for injections. In particular, the skin samples used were from the abdomen regions of (i) 16 yr old caucasian male with BMI of 20.6, and (ii) 83 yr old caucasian female with BMI of 33.5. The thickness of both the skin samples was variable according to the excision depth and exact location on the sample, but typically varied between 2 and 5 mm for the dermal tissue and 5–15 mm for the adipose tissue.

* Corresponding author.
E-mail address: jeremy.marston@ttu.edu (J. Marston).
[1] Present affiliation: North Carolina State University.
[2] Present affiliation: Intel Corporation.

https://doi.org/10.1016/j.jddst.2023.104640
Received 27 February 2023; Received in revised form 20 May 2023; Accepted 5 June 2023
Available online 9 June 2023

All skin samples were stored in a freezer at −20 °C and thawed completely prior to use. The skin samples were then weighed both before and after injection, to estimate the change in mass due to injection ($M_{ej} - M_{rejected}$), where M_{ej} is the mass of liquid expelled by the injector, and $M_{rejected}$ is the mass of liquid rejected by the skin. In addition, any residual liquid remaining on the skin surface was absorbed using filter paper to verify the mass measurements and give a corresponding estimate of the injection volume. This results in a useful measure of efficacy - namely - injection efficiency, defined as follows:

$$\eta = \frac{(M_{ej} - M_{rejected})}{M_{ej}} \times 100 \quad (1)$$

Device and loading protocol: A spring-powered device (Bioject ID Pen, see Fig. 1(a)) was used to perform jet injections with ejection volume set to $V = 100$ μL. The orifice diameters of the nozzles selected for this study were in the range $d_o = 165 - 174$ μm, leading to jet speeds of $v_j = 127 - 144$ m/s, based upon the plunger speeds in the main cartridge barrel and applying mass conservation. The shape of the nozzle tip was varied by either using the un-modified cartridge nozzle (labelled 'normal'), tapering to a point (either parabolic or conical, labelled 'tapered'), or using a modified spacer ring filled with resin (labelled 'wide'). These are shown graphically in Fig. 1(b). The modifications varied the diameter of the nozzle tips from 1 mm to 4 mm–15 mm, thus varying the contact area between the nozzle and the skin surface from ≈ 0.008 cm^2 (conical) to 1.77 cm^2 (widened).

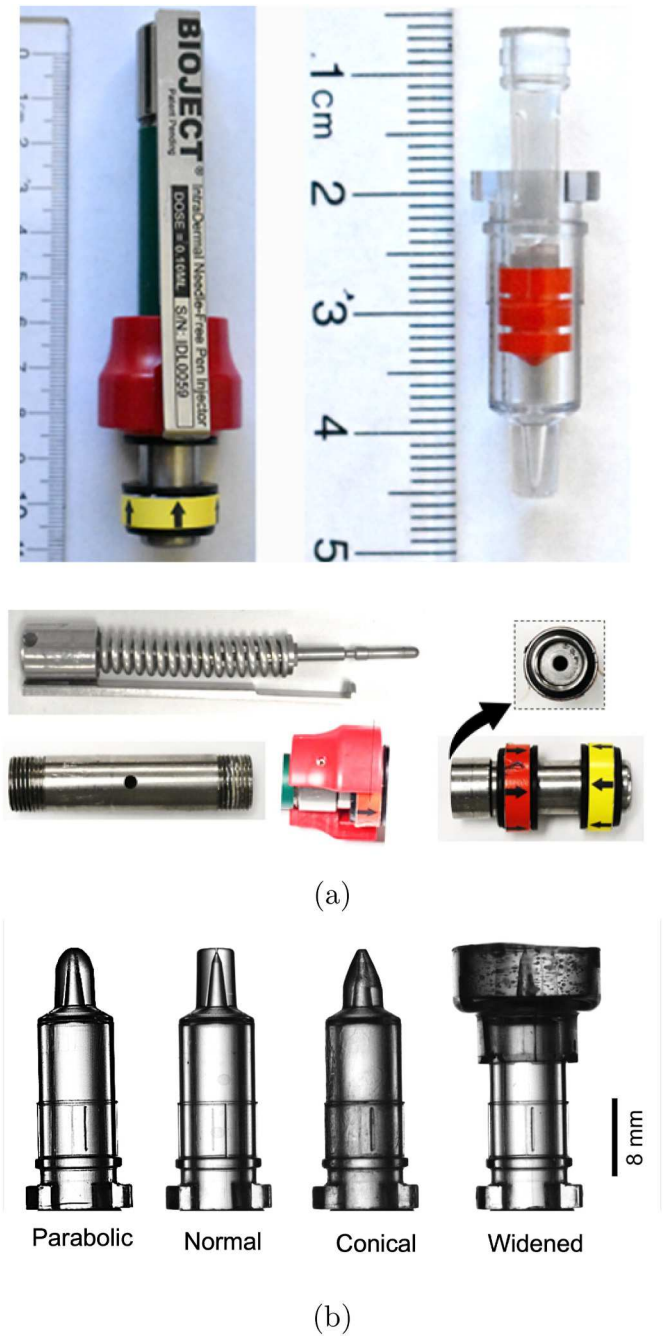

Fig. 1. (a) Bioject ID Pen injector and (b) Modified cartridge nozzles. All inner dimensions were unaltered with main cartridge inner diameter of 4.57 mm, and nozzle orifices of 165–174 μm.

To further vary the stress within the target tissues prior to injection, the skin samples were placed either on a solid glass plate, or 2 cm of pork tissue, and the nozzle tip was either just placed on the skin (zero load, to serve as the control, i.e., no pre-stressing of the tissue) or pressed into the skin with 1 kg of load, as measured by a mass balance placed underneath the tissues. The use of 1 kg load was guided by our previous study which indicated this load gave optimal injections efficiencies (see Rohilla et al. [40] for more details.

Imaging and characterization: To visualize the dispersion of liquids in the skin samples, Trypan Blue (Sigma Aldrich) was added to DI water at a concentration of 1 mg/ml. DI water was chosen as the injectate to represent low-viscosity solutions. After injection, skin samples were frozen to −4 °C, and then cut along the cross-section of the injection site to visualize the intradermal bleb, whose dimensions (depth, H, and width, D) were measured using image processing in Matlab (see Fig. 7 for an example). The injections could then be characterized in terms of the bleb dimensions, injection efficiency, η, and the amounts of injectate remaining in the dermis and fat, respectively.

3. Results and discussion

Fig. 2 shows side-by-side comparisons of representative injections into human skin (BMI 33.5) for a range of conditions. As evidenced by the lack of bleb formation in the top row, injections performed without loading (i.e., injector nozzle just placed onto skin) were mostly unsuccessful, with just a small amount of liquid injected into the very top layer of the dermal tissues. However, upon inspection of the bottom row of images, it is clear that the addition of 1 kg load has a pronounced effect - depending on the nozzle type. For the case of the tapered nozzle (Fig. 2 (a), bottom row), the injection still fails with only a small amount of dye in the dermal tissues. However, for the cases of the regular and widened nozzles (Fig. 2(b) and (c), bottom row), both the amount of liquid injected and the size of the intradermal bleb is significantly increased. Moreover, we observe that the bleb becomes slightly wider and shallower as the width of the nozzle increases. Furthermore, for injections performed with the regular and wide nozzles at 1 kg load, we observe some dye in the subcutaneous fat tissue. Since there is no visible jet path into this tissue, we conclude it is diffusion from the primary deposit in the dermal tissues. For the injections in Fig. 2, the substrate backing the skin samples was glass (i.e., rigid), whilst the average thicknesses of the dermal and fat tissues were ~2 mm and ~11 mm, respectively. It is noteworthy that the effect of nozzle shape and load herein results in a similar qualitative effect as varying jet speed in McKeage et al. [25], where low jet speeds ($V_j \leq 90$ m/s) led to only superficial deposit of very small volumes in the dermis, while higher jet speeds ($V_j > 100$ m/s) led to larger delivery volumes in the sub-cutaneous and intramuscular tissues.

At a qualitative level, the failed injections for those performed without loading can be explained by considering the interaction of the jet with the skin substrate, as follows: When no loading is applied, the momentum of the jet can be sufficient to cause a large deformation (dimple) in the surface, increasing the distance between the orifice and the skin surface. This offset, coupled with the compliance of the fat tissue leads to the jet being deflected from the surface and reduces the

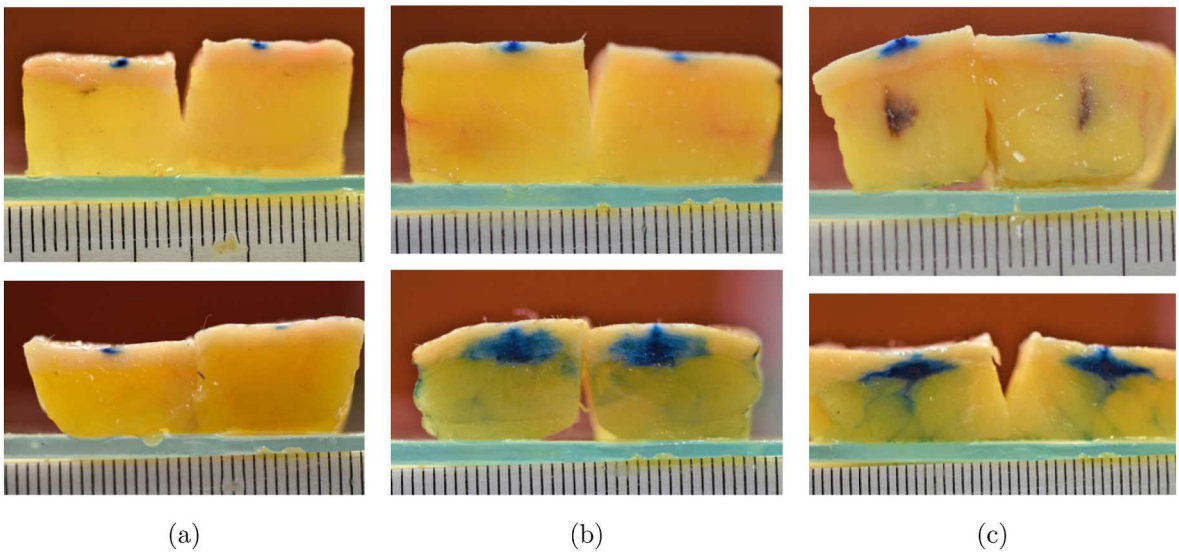

Fig. 2. Medial sections of injection sites for human skin with (a) tapered, (b) normal, and (c) widened nozzles at 0 kg (top row) and 1 kg (bottom row) loading. BMI = 33.5, average dermal thickness 2 mm, fat tissue thickness 10–11 mm. The scale divisions in each image are millimetric. Each image shows both sides of the cut.

penetration and delivery of liquid into the tissue [43]. This effect is seen to varying degrees depending upon the thickness of both the dermal and fat tissues, and their corresponding stiffness. At a more quantitative level, the puncture of a substrate by a liquid jet could be characterized by a threshold jet Weber number based upon the modulus of the substrate, as per the approximations derived by van der Ven et al. [44], where the threshold for elastic/plastic deformation was given as $We_{jet} = 0.728G^{0.83}$, where G is the stiffness. Using the values for the shear modulus derived from Baxter & Mitragotri [29] of $G \approx 500$ kPa for human skin, their empirical equation yields $We_{jet} = 39100$, which is very close to the jet Weber numbers in this study ($We_{jet} = \rho d_o V_j^2 / \sigma = 38,800 - 47,600$), indicating a highly elastic response, in agreement with the reasoning above.

In the specific case of Fig. 2 (with high BMI) the thickness of the fat tissue relative to the dermis ($\sim$ 11 mm vs $\sim$ 2 mm) could also be a factor leading to failed injections. This becomes apparent when compared to injections performed into a different skin sample with less fat tissue (and higher ratio of dermis:fat). The corresponding images for this skin are shown in Fig. 3, where the difference between the two rows is less significant than Fig. 2. The major discernible difference between zero applied load (top row) and 1 kg of applied load (bottom row) is the increased amount of dye present in the fat tissue for the loaded injections, which was also observed in Fig. 2. In this instance, we also observe a slight increase in lateral dispersion (i.e., increased bleb width), but we do not observe a significant effect of the nozzle shape on injection efficiency.

A summary of the injection efficiencies of the configurations shown in Figs. 2 and 3 is presented in Fig. 4 (a) and (b), respectively. This quantitative assessment depicts the qualitative findings in the raw images, namely, unsuccessful or failed injections for the skin with low dermis:fat ratio and 0 kg load, but a significant improvement when under 1 kg of load. However, this was only consistently observed for the normal and wide nozzle shapes, not for the tapered nozzle. We hypothesize that the tapered shapes, with a much smaller contact area ($d \approx$ 1 mm), leads to a highly localized stress that significantly compresses the skin and fat tissues above a threshold such that the tissue layers are too narrow in the immediate vicinity of the orifice; When the stress within the target tissue is too high, the fluid cannot penetrate and disperse laterally, due to the high counter-pressure from the tissue [45]. A previous study [29] reported that the average Young's modulus of human skin is around 0.3 MPa, which would require a critical 'erosion stress' of approximately 0.5–1 MPa, typically supplied by the jet in the form of inertial pressure, $\frac{1}{2}\rho v_j^2 \sim O(10)$ MPa in order to puncture.

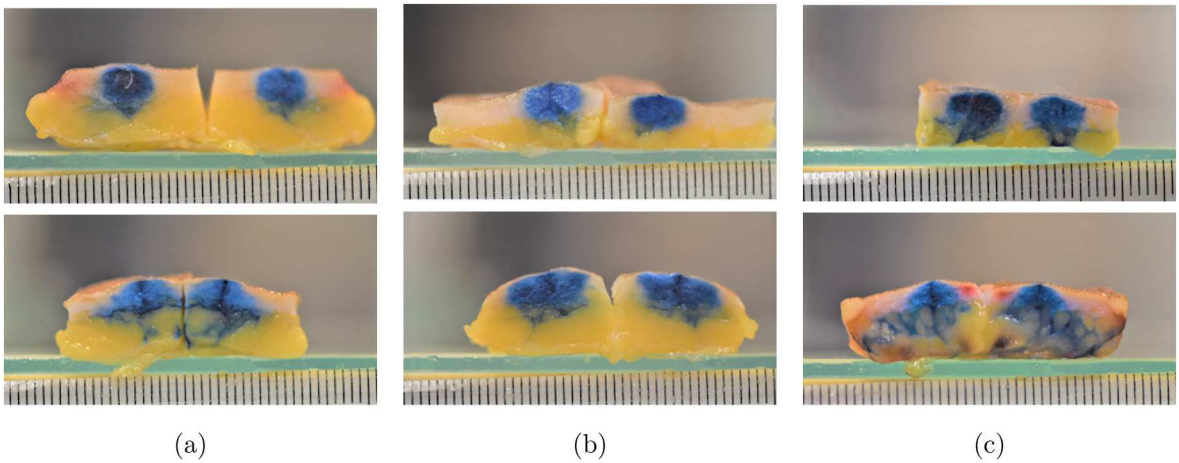

Fig. 3. Medial sections of injection sites for human skin with (a) tapered, (b) normal, and (c) widened nozzles at 0 kg (top row) and 1 kg (bottom row) loading. BMI = 20.6, average dermal thickness 3–4 mm, fat tissue thickness 6–8 mm. The scale divisions in each image are millimetric. Each image shows both sides of the cut.

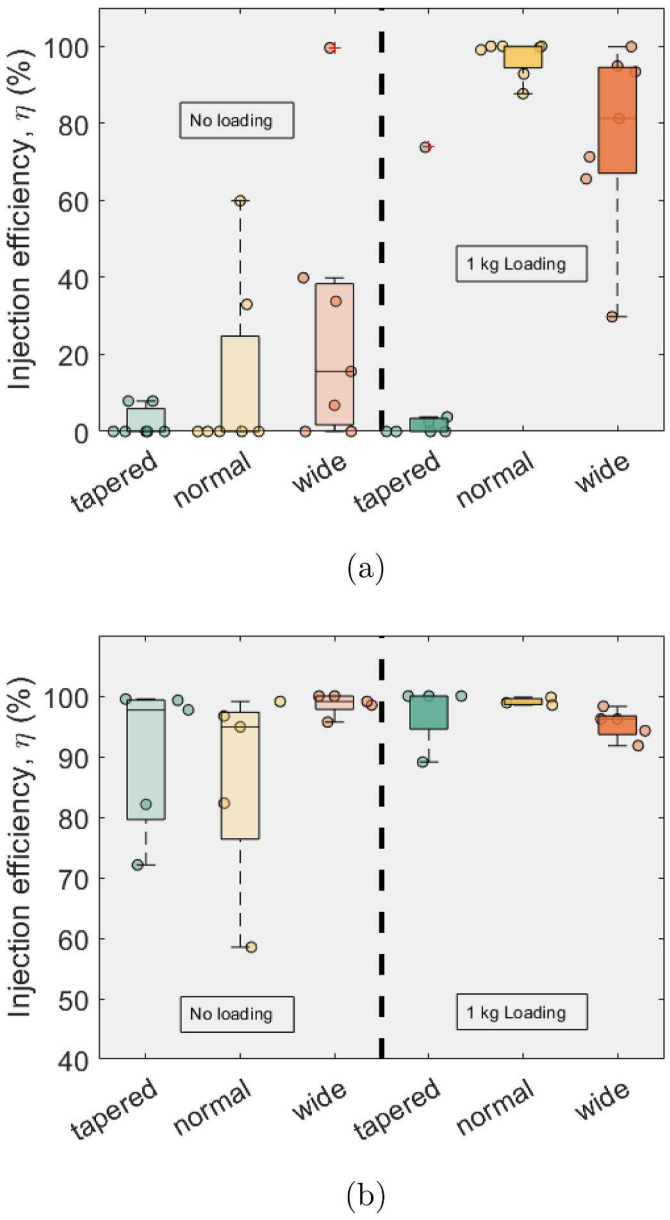

Fig. 4. Summary data of injection efficiency into human skin backed by rigid (glass) substrate. (a) BMI = 33.5 (corresponding to the skin in Fig. 2), and (b) BMI = 20.6 (corresponding to the skin in Fig. 3).

However, since the jet interacts with the tissues (i.e. erosion during the puncture and penetration, and diffusion during the deposition stage), there is a high degree of momentum dissipation reducing the total penetration depth. When additional loading is used, the skin tissues are compressed, and we estimate the magnitude and distribution of this stress in the simplest framework of contact mechanics simply from the normal load and approximate cylindrical contact area. For example, the tapered nozzles with flat tips and contact diameter of 1 mm and 1 kg load ($F = 9.81$ N) would result in a stresses of $O(10)$ MPa, which then becomes comparable to the jet inertial pressure, resulting in failed injections. In contrast, the application of the same 1 kg load with larger nozzle shapes (normal, $d = 4.2$ mm, and wide, $d = 15$ mm) promotes a more uniform distribution of stress within the skin tissue, reducing local counter-pressure [45] to the jet flow, leading to more successful injections. A simple proxy visualization of the stress distribution can be provided by the contact pressure versus radius, based on Hertz contact theory with $p(r) = p_0(1 - r^2/R^2)^{1/2}$, with $P_0 = F_N/(2A)$, where F_N is the normal load force and A is the contact area. This function is shown in Fig. 5 for the tip diameters of 1 mm, 4.2 mm, and 15 mm, respectively.

We also note that the Young's modulus of human skin is reported to increase linearly with age, with skin becoming thinner and stiffer [46], which also helps to explain the discrepancy between our injection efficiencies in the two skin samples, given that the skin sample from the older patient showed reduced injection efficiency.

For the injections into the lower BMI skin tissue (higher ratio of dermal:fat thickness, as per Fig. 4(b)), we do not observe a significant improvement in terms of mean injection efficiency, rather an improved consistency. This is evident from the narrow data ranges (tighter grouping of data points) observed for 1 kg load. In this case, as argued above, we postulate this is due to reduced tissue compliance, i.e., reduced elastic response (from less fat tissue) coupled with load that prestresses the skin. Surprisingly, even the tapered nozzle resulted in improved performance for this low BMI skin, which implies that the skin thickness and ratio of dermal to fat thickness is perhaps an equally important factor as the load itself.

To render more realistic trials, a supplemental set of injections were conducted with a 2-cm-thick section of pork tissue placed under the skin. Due to the availability of skin samples, these trials could only be conducted with the lower BMI sample. The data for these trials are shown in Fig. 6. For purposes of comparison, the left side of the plot replicates the data from Fig. 4(b) for glass backing, whilst the pork tissue backing is on the right. Here, we observe a decrease in injection efficiency for the tapered and normal nozzles ($\bar{\eta}$: 97→90%, $\bar{\eta}$: 99→90%), and a marginal (but non-significant) increase for the wider nozzle, with $\bar{\eta}$: 95→98% for glass backing versus pork tissue backing. For the tapered and normal nozzles, the fact that $\bar{\eta}$ decreases and the spread increases is consistent with the reasoning that more tissue compliance decreases overall injection success rates.

As per the qualitative observations in Figs. 2 and 3, the injection dispersion patterns can vary significantly. Therefore, to further quantify the injections, we also measured the bleb dimensions and total area coverage (via filtering and binarizing) to determine the approximate percentage of injectate in the dermis and fat tissues, respectively. Fig. 7 shows an example of the image analysis performed to determine the extent of the bleb, and location of boundary between the dermal and fat tissues. A simple count of pixels above/below the boundary then yields the percentage of injected fluid in either tissue. In this realization, the approximate amount of injectate in the dermis is 68%, with 32% reaching the fat tissue.

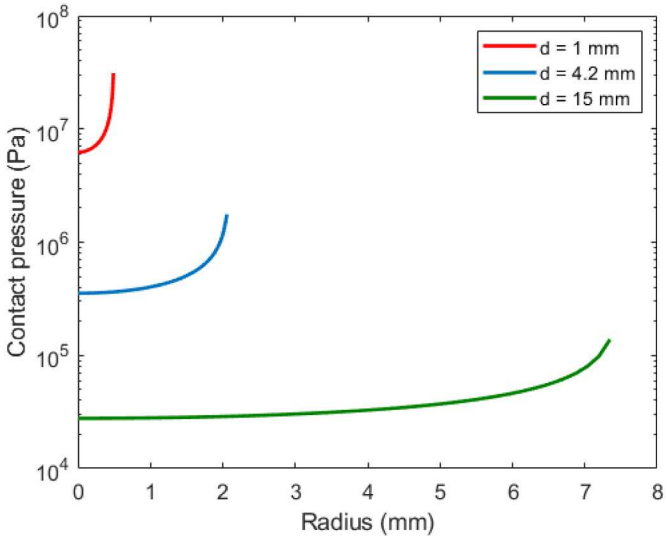

Fig. 5. Contact pressure, $p(r)$, versus radius for different nozzle diameters with normal load of 1 kg.

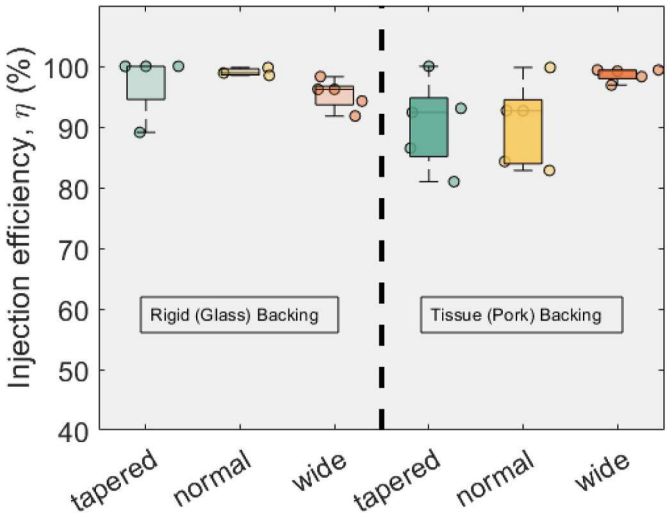

Fig. 6. Comparison of injection efficiencies into human skin with rigid vs. tissue backing.

Performing these analyses across multiple sets of images yields the ensemble data in Fig. 8, which is segmented into (i) glass backing without load, (ii) glass backing with 1 kg load, and (iii) pork tissue backing with 1 kg load. The data exhibits significant intra-sample variation, which could be partly attributed to heterogeneity in the skin, but the overall trends indicate that there is no significant effect of loading/backing for the tapered or normal nozzles, with p-values $p > 0.1$ in both cases, whilst there is a significant effect of the loading/backing for the wide nozzle ($p < 0.05$). In particular, the data for the wide nozzle with 1 kg load on rigid backing shows a reduction in the amount remaining in the dermis to around 20–40% compared with the other configurations with around 60–80%. We hypothesize that this is due to the compression of the skin between the nozzle tip and the rigid glass plate forcing more liquid into the fat tissue. This effect would then not be significant in the other configurations (i.e., no loading and tissue-backed skin samples), yielding the higher percentages in the dermis in those cases.

Focusing on the most relevant configuration, i.e. injections with applied load onto human skin samples backed by pork tissue, to simulate real-life injections, the bleb dimensions are presented in Fig. 9. Note that for the purposes of this analysis, the bleb dimensions are taken to be those of the primary (connected) deposit, i.e., discounting the 'finger-like' diffusion into fat tissue. Here we find that the intradermal blebs are consistently around 4–5 mm deep in all cases, but the width of the dispersion varies significantly; specifically, the wider nozzle produces a more consistent and wider bleb, around 7–8 mm in diameter, yielding width-to-depth aspect ratios of $D/H \approx 1.5 - 2$. Again, we attribute this to the uniform stress in the dermis, which has a reduced apparent thickness due to the compression, leading to the fluid being forced to disperse more laterally.

From a clinical perspective, if an intradermal injection is to be augmented with electroporation (EP), which can significantly improve immune response for DNA vaccination [41,42], it is beneficial to have a shallow and broad dispersion. In other words, wider but less deep so that the electrical current can more easily permeate the tissue to enable the EP to take place, and the drug or vaccine can ultimately transfect more cells. In this regard, the use of a wide contact area with applied load achieves the desired outcome, as evident from the bleb dimensions, presented in Fig. 9.

4. Conclusions

Whilst the results of this study indeed make a case for the effects of

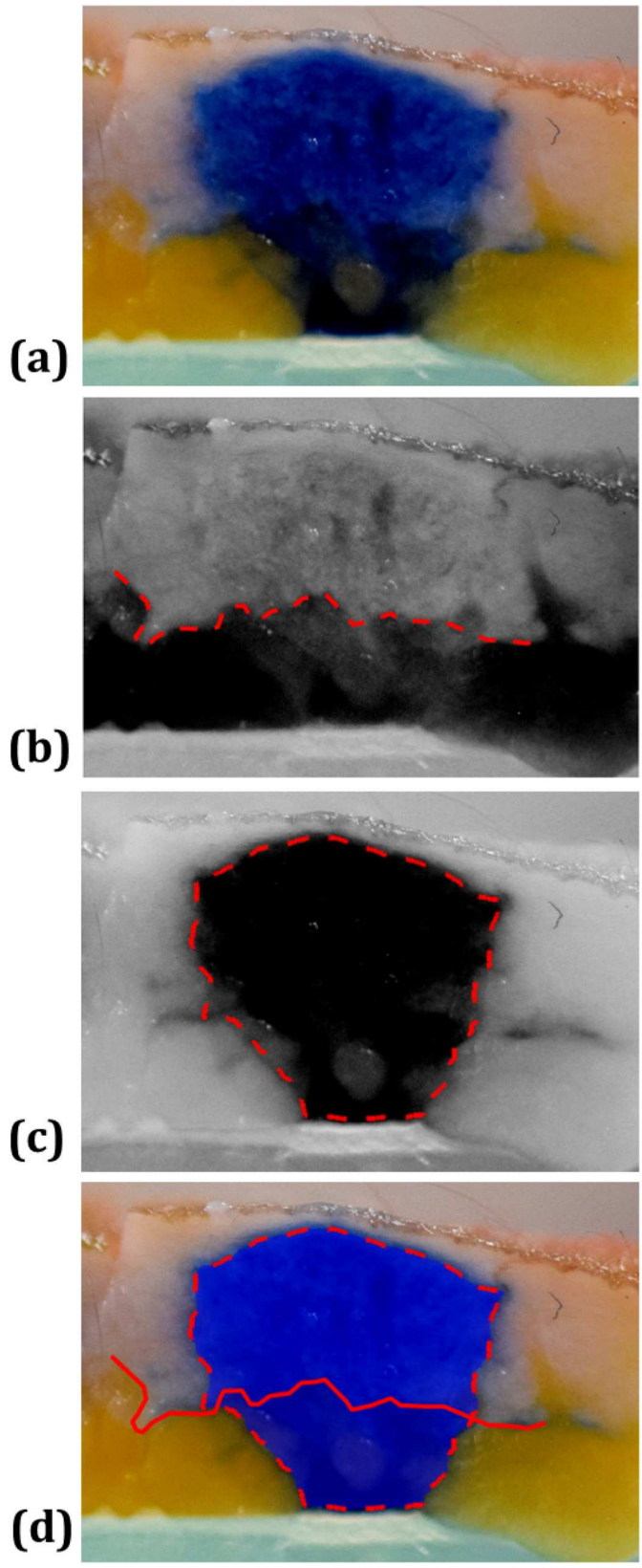

Fig. 7. Image analysis performed on blebs to determine approximate percentage of injectate in dermal and fat tissues. (a) Original color image cropped around injection site; (b) Blue channel filter with location of boundary between dermis and fat tissues; (c) Red channel filter with outline of bleb; (d) Artificially filled outline overlayed on original with the location of tissue boundary. (For interpretation of the references to color in this figure legend, the reader is referred to the Web version of this article.)

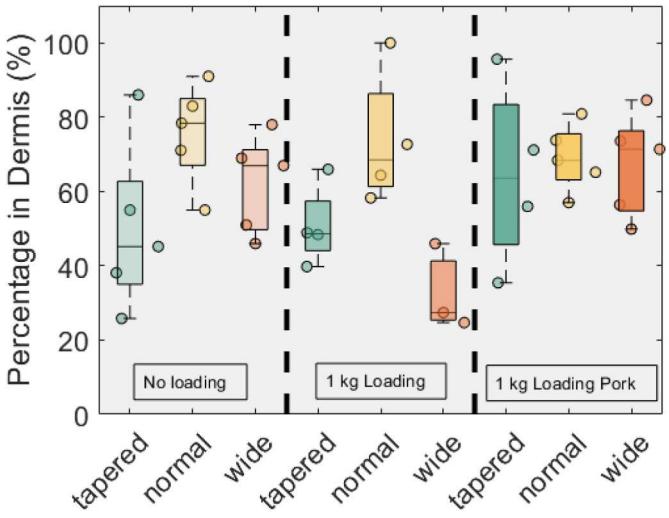

Fig. 8. Comparison of injection efficiencies into human skin (BMI = 20.6) with rigid vs. tissue backing.

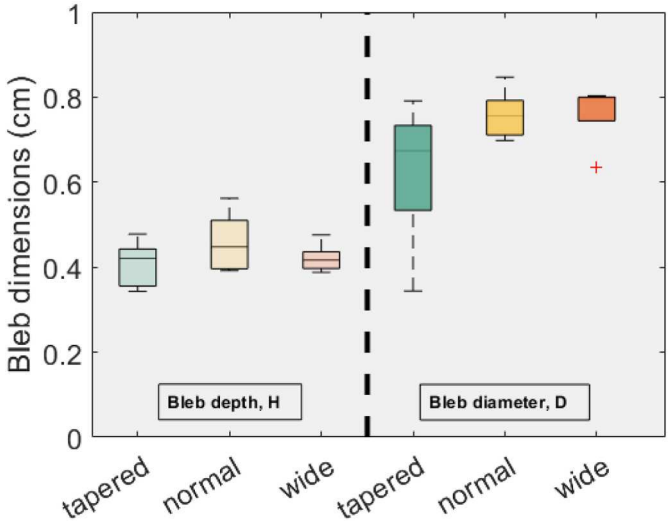

Fig. 9. Bleb dimensions (depth and width) for injections into human skin with 1 kg load and pork tissue backing. Red cross indicates an outlier. (For interpretation of the references to color in this figure legend, the reader is referred to the Web version of this article.)

nozzle shape and applied load, and multiple repeat trials were performed in attempt to rule out any significant errors, we must acknowledge several limitations of the experimental procedures and analyses.

1. Due to variation in orifice diameter (165–174 μm), there are variations in jet speeds (from 127 to 144 m/s) between the different nozzle types used.
2. The injection efficiencies are based upon an average of both the skin mass (before vs. after injection) and filter papers used to blot undelivered liquid from the skin surface. However, any fluid that is absorbed into the skin but not actually delivered via the puncture by the jet is not accounted for.
3. Our study only used one target injection volume (100 μL) as per fractional dose skin vaccination guidelines. However, increasing volume has been shown to increase both penetration depth and dispersion width [24,28], therefore replicating this study (i.e., effects of applied load combined with ampule contact shape) with increased volumes may be of interest for applications targeting larger volumes for skin or subcutaneous delivery.
4. The bleb dimensions are based on the medial section chosen, and cannot account for dispersion in the direction perpendicular to this plane. It is also unclear how much fluid reaches the fat tissue due to jet penetration or simply via diffusion post-injection. Thus for future studies, a combination of high-speed X-ray and micro-computed tomography (μ-CT) imaging would be preferable for a complete understanding of jet dynamics and liquid distribution.
5. The skin samples used exhibited heterogeneity in terms of local fat tissue thickness, meaning that even though care was taken to control sources of variation in the experiments, some inherent variation occurred due to skin properties (tension, dermis and fat thickness).

Optimizing injector parameters (speed, orifice diameter, load, etc.) for skin-based injections or deeper subcutaneous or intramuscular injections is crucial for needle-free injectors in order to improve injection efficiency (correct delivery to the target tissue) and ultimately health outcomes. Our limited study herein indeed shows that both the shape of the nozzle (ampule) tip and the load with which it is pressed onto the skin can have a significant effect. We postulate that our findings here can be replicated in other needle-free injectors using different actuation mechanisms. For intradermal injections, our results indicate that a wider tip with approximately 1 kg of load can improve consistency and promote superior dispersion characteristics, which may be beneficial for EP-assisted injections into skin.

Author statement

Jeremy Marston and Yatish Rane conceived the project and designed the experiments. Cormak Weeks, Whitney Tran and Yatish Rane performed the experiments and raw data analyses. Jeremy Marston performed secondary data analyses and reduction, and wrote and revised the manuscript.

Declaration of competing interest

The authors declare that they have no known competing financial interests or personal relationships that could have appeared to influence the work reported in this paper.

Data availability

Data will be made available on request.

Acknowledgments

This work was financially supported by The National Science Foundation via award CBET-1749382. We would like to thank Department of the Animal Sciences at Texas Tech for tissue from porcine cadavers, and Inovio Pharmaceuticals for the Bioject ID Pen devices. We also acknowledge early discussions on the main concept of this work with Paul Fisher and Jay McCoy from Inovio Pharmaceuticals.

References

[1] S. Mitragotri, Current status and future prospects of needle-free liquid jet injectors, Nat. Rev. Drug Discov. 5 (2006) 543–548.
[2] Y. Nir, A. Paz, E. Sabo, J. Potasman, Fear of injection in young adults: prevalence and associations, Am. J. Trop. Med. Hyg. 68 (2004) 341–344.
[3] G.H. Verrips, R.A. Hirasing, M. Fekkes, T. Vogels, S.P. Verloove-Vanhorick, H. A. Delemarre-Van de Waal, Psychological responses to the needle-free Medi-Jector or the multidose Disentronic injection pen in human growth hormone therapy, Acta Paediatr. 87 (1998) 154–158.
[4] A. Kane, J. Lloyd, M. Zaffran, L. Simonsen, M. Kane, Transmission of hepatitis B, hepatitis C and human immunodeficiency viruses through unsafe injections in the developing world: model-based estimates, Bull. WHO 77 (1999) 801–807.
[5] The World Health Report 2002: Reducing Risks, Promoting Healthy Life.

[6] A. Mannocci, G. De Carli, V. Di Bari, R. Saulle, B. Unim, N. Nicolotti, L. Carbonari, V. Puro, G. La Torre, How much do Needlestick injuries cost? A systematic review of the economic evaluations of needlestick and sharps injuries among healthcare personnel, Infect. Control Hosp. Epidemiol. 37 (2016) 635–646.
[7] J. Jagger, E.H. Hunt, R.D. Pearson, Estimated cost of needlestick injuries for six major needled devices, Infect. Control Hosp. Epidemiol. 11 (1990) 584–588.
[8] L. Jodar, P. Duclos, J.B. Milstein, E. Griffiths, M.T. Aguado, C.J. Clements, Ensuring vaccine safety in immunization programmes - a WHO perspective, Vaccine 19 (2001) 1594–1605.
[9] M.T. Yousafzai, A.F. Saleem, O. Mach, A. Baig, R.W. Sutter, A.K.M. Zaidi, Karachi, Pakistan, Heliyon, in: Feasibility of Conducting Intradermal Vaccination Campaign with Inactivated Poliovirus Using Tropis Intradermal Needlefree Injection System, vol. 3, 2017, e00395.
[10] J. Hickling, R. Jones, Intradermal Delivery of Vaccines: A Review of the Literature and the Potential for Development for Use in Low- and Middle-Income Countries *WHO Report*, 2009.
[11] A. Bavdekar, J. Oswal, P.V. Ramanan, et al., Immunogenicity and safety of measles-mumps-rubella vaccine delivered by disposable-syringe jet injector in India: a randomized, parallel group, non-inferiority trial, Vaccine 36 (2018) 1220–1226.
[12] J.K. Simon, C. Michaela, M.F. Pasetti, et al., Safety, tolerability, and immunogenicity of inactivated trivalent seasonal influenza vaccine administered with a needle-free disposable syringe jet injector, Vaccine 29 (2011) 9544–9550.
[13] B.S. Graham, M.E. Enama, M.C. Nason, et al., DNA vaccine delivered by a needle-free injection device improves potency of priming for antibody and CD8+ T-Cell responses after rAd5 boost in a randomized clinical trial, PLoS One 8 (2013), e59340.
[14] W. Walther, U. Stein, I. Fichtner, et al., Nonviral jet injection gene transfer for efficient in vivo cytosine deaminase suicide gene therapy of colon carcinoma, Mol. Ther. 12 (2005) 1176–1184.
[15] R.L. Brocato, S.A. Kwilas, M.D. Josleyn, et al., Small animal jet injection technique results in enhance immunogenecity of hantavirus DNA vaccines, Vaccine 39 (2021) 1101–1110.
[16] J.J. Suschak, S.L. Bixler, C.V. Badger, et al., A DNA vaccine targeting VEE virus delivered by needle-free jet injection protects macaques against aerosol challenge, npj Vaccines 7 (2022) 46.
[17] S. Resik, A. Tejeda, O. Mach, et al., Needle-free jet injector intradermal delivery of fractional dose inactivated poliovirus vaccine: association between injection quality and immunogenicity, Vaccine 33 (2015) 5873–5877.
[18] C. Daly, N.A. Molodecky, M. Sreevatsava, et al., Needle-free injectors for mass administration of fractional dose inactivated poliovirus vaccine in Karachi, Pakistan: a survey of caregiver and vaccinator acceptability, Vaccine 38 (2020) 1893–1898.
[19] A.J. Mohammed, S. Al-Awaidy, S. Bawikar, et al., Fractional doses of inactivated poliovirus vaccine in Oman, N.E. J. Med. 365 (2010) 2351–2359.
[20] D. Soonawala, P. Verdijk, Wijmenga-Monsuur, C.J. Boog, P. Koedam, L.G. Visser, N.Y. Rots, Intradermal fractional booster of inactivated poliomyelitis vaccine with a jet injector in healthy adults, Vaccine 31 (2013) 3688–3694.
[21] J. Schramm-Baxter, S. Mitragotri, Needle-free jet injections: dependence of jet penetration and dispersion in the skin on jet power, J. Contr. Release 97 (2004) 527–535.
[22] J. Schoppink, D. Fernandez-Rivas, Jet injectors: perspectives for small volume delivery with lasers, Adv. Drug Deliv. Rev. 182 (2022), 114109.
[23] J. Schramm, S. Mitragotri, Transdermal drug delivery by jet injectors: energetics of jet formation and penetration, Pharma Res. 19 (11) (2002) 1673–1679.
[24] D. Zeng, N. Wu, L. Xie, X. Xia, Y. Kang, An experimental study of a spring-loaded needle-free injector: influence of the ejection volume and injector orifice diameter, J. Mech. Sci. Technol. 33 (11) (2019) 5581–5588.
[25] J.W. McKeage, B.P. Ruddy, P.M.F. Nielsen, A.J. Taberner, The effect of jet speed on large volume jet injection, J. Contr. Release 280 (2018) 51–57.
[26] P. Rohilla, Y.S. Rane, I. Lawal, et al., Characterization of jets for impulsively-started needle-free jet injectors: influence of fluid properties, J. Drug Deliv. Sci. Technol. 53 (2019), 101167.
[27] P. Rohilla, J.O. Marston, In-vitro studies of jet injections, Int. J. Pharm. 568 (2019), 118503.
[28] J. Schramm-Baxter, J. Katrencik, S. Mitragotri, Jet injection into polyacrylamide gels: investigation of jet injection mechanics, J. Biomech. 37 (2004) 1181–1188.
[29] J. Baxter, S. Mitragotri, Jet-induced skin puncture and its impact on needle-free jet injections: experimental studies and a predictive model, J. Contr. Release 106 (2005) 361–373.
[30] Y.S. Rane, J.O. Marston, Computational study of fluid flow in tapered orifices for needle-free injectors, J. Contr. Release 319 (2020) 382–396.
[31] Y.S. Rane, J.O. Marston, Transient modelling of impact driven needle-free injectors, Comput. Biol. Med. 135 (2021), 104586.
[32] T.S. Hansen, Nozzle Device with Skin Stretching Means, A1, US Patent 0021716, 2007.
[33] J.B. Slate, L.A. Gorton, M.W. Burk, Jet Injector, A1, European Patent, 2002, 1161961.
[34] J.B. Slate, M.W. Burk, L.A. Gorton, Needleless jet injector system with separate drug reservoir, US Patent 55707 (2002) A1.
[35] J.B. Slate, M.W. Burk, L.A. Gorton, Needleless jet injector system with separate drug reservoir, US Patent 6 (2003), 652,483 B2.
[36] J.B. Slate, M.W. Burk, L.A. Gorton, Sequential Impulse/delivery Fluid Medicament Injector, A1, US Patent 0059286, 2003.
[37] L. Bik, A. Wolkerstorfer, V. Bekkers, et al., Needle-free jet injection-induced small-droplet aerosol formation during intralesional bleomycin therapy, Laser Surg. Med. 54 (2021) 572–579.
[38] C. Cappello, M. Wixey, J.W. Bingham, Needle-free Intradermal Injection Device, A1, US Patent 0150820, 2013.
[39] C. Cappello, M. Wixey, J.W. Bingham, Needle-free Injection Device, US Patent 9408972 B2, 2016.
[40] P. Rohilla, I. Lawal, A. Le Blanc, et al., Loading effects on the performance of needle-free jet injections in different skin models, J. Drug Deliv. Sci. Technol. 60 (2020), 102043.
[41] K.E. Broderick, L.M. Humeau, Electroporation-enhanced delivery of nucleic acid vaccines, Expert Rev. Vaccines 14 (2015) 195–204.
[42] F. Lin, X. Shen, J. McCoy, et al., A novel prototype device for electroporation-enhanced DNA vaccine delivery simultaneously to both skin and muscle, Vaccine 29 (39) (2019) 6771–6780.
[43] Y.S. Rane, J.B. Thomas, P. Fisher, K.E. Broderick, J.O. Marston, Feasibility of using negative pressure for jet injection applications, J. Drug Deliv. Sci. Technol. 63 (2021), 102395.
[44] D. van der Ven, D. Morrone, M.A. Quetzeri-Santiago, Fernandez-Rivas, Microfluidic jet impact: spreading, splashing, soft substrate deformation and injection, it J. Colloid & Interface Sci. 636 (2023) 549–558.
[45] Md Shahriar, A. Rewanwar, P. Rohilla, J. Marston, Understanding the effect of counterpressure buildup during syringe injections, Int. J. Pharm. 602 (2021), 120530.
[46] M. Pawlaczyk, M. Lelonkiewicz, M. Wieczorowski, Age-dependent biomechanical properties of the skin, Postepy Dermatol. Alergol. 30 (5) (2013) 302–306.